Separation Science and Technology
Publication details, including instructions for authors and subscription information:
http://www.informaworld.com/smpp/title~content=t713708471

FRACTIONATION OF ^{15}N IN COUNTERCURRENT HNO_3-NO SYSTEM AT LOW TEMPERATURE

Mikhail S. Safonov[a]; Vladimir I. Gorshkov[a]; Vladimir A. Ivanov[a]; Nikita E. Tamm[a]
[a] Chemical Department, Lomonosov Moscow State University, Moscow, Russia

Online publication date: 30 July 2001

To cite this Article Safonov, Mikhail S. , Gorshkov, Vladimir I. , Ivanov, Vladimir A. and Tamm, Nikita E.(2001) 'FRACTIONATION OF ^{15}N IN COUNTERCURRENT HNO_3-NO SYSTEM AT LOW TEMPERATURE', Separation Science and Technology, 36: 8, 1991 — 2025
To link to this Article: DOI: 10.1081/SS-100104765
URL: http://dx.doi.org/10.1081/SS-100104765

SEPARATION SCIENCE AND TECHNOLOGY, 36(8&9), 1991–2025 (2001)

FRACTIONATION OF ^{15}N IN COUNTERCURRENT HNO_3-NO SYSTEM AT LOW TEMPERATURE

Mikhail S. Safonov, Vladimir I. Gorshkov, Vladimir A. Ivanov,* and Nikita E. Tamm

Chemical Department, Lomonosov Moscow State University, Moscow 119899 Russia

ABSTRACT

This article describes the method for fractionation of ^{15}N isotope based on the exchange of nitrogen isotopes in the system consisting of liquid mixtures of nitric acid and nitrogen oxides and the gaseous nitrogen oxide in the temperature range between 233 and 263 K under atmospheric pressure developed by the authors. The chemical interactions occurring between liquid nitric acid and gaseous nitrogen oxide at low temperatures and the equilibrium of the nitrogen isotopes exchange has been studied by means of the analysis of each co-existing phase in a packed column with counter-current movement of liquid and gas phases. The results obtained by theoretical modeling and experimental testing of the experimental plant have allowed one to conclude that the low temperature NITROX method is promising for the large-scale ^{15}N production. This method improves upon the main technological parameters of the process as compared to traditional room temper-

*Corresponding author.

ature NITROX system. It allows for increasing the productivity of the same column and the degree of ^{15}N extraction from the feed nitric acid up to two times, and for decreasing almost twice the consumption of sulphur dioxide (which is used to convert HNO_3 to NO).

INTRODUCTION

Nitrogen of natural abundance contains only 0.365% of ^{15}N. The heavy nitrogen isotope, ^{15}N, has been widely used for decades in biochemical, medical, agricultural, and environmental research. Moreover, the highly enriched ^{15}N has been considered a promising component of the breeder reactor fuel materials due to its favorable nuclear properties (1). The need to increase significantly the production of ^{15}N stimulates the interest to developing new and efficient large-scale nitrogen isotopes fractionation processes.

The highly enriched ^{15}N is mainly produced by using the NITROX process developed by Spindel and Taylor (2,3), which is based on the chemical exchange between liquid nitric acid and gaseous nitrogen oxide according to the following reaction:

$$^{15}NO + H^{14}NO_3 = {}^{14}NO + H^{15}NO_3 \quad (1)$$

The NITROX process was used during recent decades in industrial scale to produce highly enriched isotope N^{15} (4–13). For the optimal concentration of nitric acid of 10 M at $T = 298$ K and atmospheric pressure reaction (1) is characterized by the separation factor $\alpha = 1.055$ (14,15). In the enriched product refluxer connected with the bottom part of the exchange column the liquid flow of nitric acid is reduced with SO_2 to the gaseous phase of an appropriate chemical composition with predomination of NO. The reaction proceeds by the following scheme:

$$2\,HNO_3 + 3\,SO_2 + 2\,H_2O = 2\,NO + H_2SO_4 \quad (2a)$$

$$2\,HNO_3 + SO_2 = 2\,NO_2 + H_2SO_4 \quad (2b)$$

The main drawback of the NITROX process is a high consumption of SO_2, which substantially increases the cost of the ^{15}N enriched product and leads to the need to discharge large volumes of ~50% sulfuric acid.

The majority of works on the development of the Spindel-Taylor method was focused on improvement of hydrodynamic characteristics of the process through optimization of the material, the shape and the dimensions of helixes used for packing of the exchange column (11,16–20), improvement of the material and the design of the refluxer (21,22), and optimization of the initial nitric acid concentration (1,5,6,16,23).

MARCEL DEKKER, INC.
270 Madison Avenue, New York, New York 10016

The NITROX separation columns usually operate at the atmospheric pressure and room temperature of ~298 K, which has been indicated by Krell et al. (17) as the optimal one. However, the authors of other early work (16) determined the optimal temperature to be 318 K, because at this temperature the composition of the gaseous mixture of nitrogen oxides in the column was identical to that of the gas flow from the refluxer. Later systematic studies (24–26) of influence of the temperature on the ^{15}N enrichment have shown that the optimum temperature is close to 318 K. Khoroshilov and Katalnikov (25,26) have also found that an increase of temperature from 283 K to 318 K results in ~ 1.2–1.4 fold decrease of SO_2 expenditure at a constant feed-flow of the initial nitric acid. However, they did not consider the influence of temperature on the degree of ^{15}N extraction from the initial nitric acid and on the productivity of separation set-up.

Simultaneous optimization of both the degree of extraction and enrichment in isotope separations along with minimization of the production costs were considered in (27–32) where the idea to use non-isothermal conditions in separation column was also originated. It was suggested to maintain a certain temperature gradient, which gradually increased along the column toward the refluxer. A lower temperature at the feed-point of the column provided a high degree of extraction of the target component from the initial mixture due to a high value of separation factor. At the same time a gradual increase of temperature in direction to the refluxer end decreased the HETS values in the main part of the column resulting in an increase of enrichment at the refluxer end of the column. The authors of this elegant idea investigated its applicability for separation of different isotope mixtures including the ^{15}N fractionation by using the NITROX-system (30–32).

This article reports the results obtained by the development of a new method for ^{15}N fractionation by exchange in the system involving the same initial reagents as those used in the NITROX process (HNO_3 and gaseous NO). The new process is also carried out under atmospheric pressure but in the temperature range from 233 to 263 K. This method was discovered for the first time in 1974 (33). The main advantage of the method is in significant decrease of the SO_2 consumption. The development of the low-temperature version of the NITROX process was based on the experimental study of 1) chemical interactions between liquid HNO_3 and gaseous NO at low temperatures; 2) equilibrium of nitrogen isotopes exchange, and 3) dynamic characteristics of the inter-phase isotope exchange in the column with counter-current of liquid and gaseous phases. The results of these studies are given below.

PRINCIPLES OF LOW-TEMPERATURE NITROX-METHOD

The flowsheet of the method is shown in Fig. 1. The set-up consists of a packed low-temperature exchange column I and its supplementary systems cou-

MARCEL DEKKER, INC.
270 Madison Avenue, New York, New York 10016

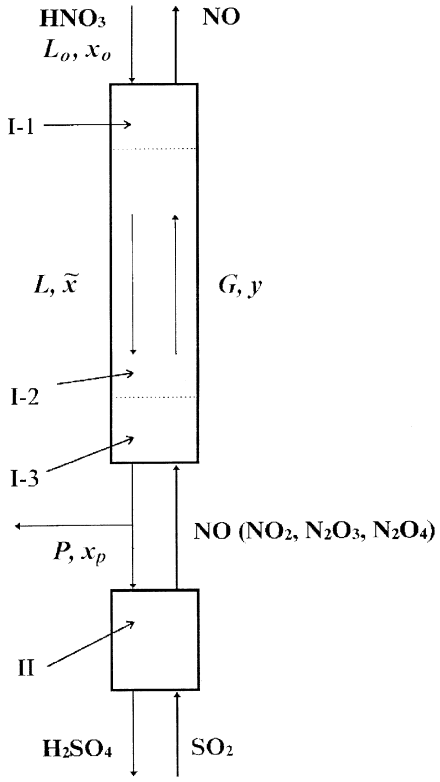

Figure 1. Flow-sheet of low-temperature NITROX method. I-1, top part of exchange column (absorption of NO by HNO_3); I-2, main part of exchange column; I-3, bottom part of exchange column (condensation of all nitrogen oxide except NO); II, refluxer (see text).

pled with the refluxer system II. The nitric acid is fed to the top of the exchange column I and the gaseous mixture of nitrogen oxides containing mainly NO is fed to its bottom from the refluxer. All nitrogen oxides (except NO) condense almost completely in the bottom part I-3 of column I and then are returned with the liquid flow back to the refluxer. Hence, in the main part I-2 of the exchange column the gas phase contains NO with the minimal admixture ($<2\%$) of other nitrogen oxides. Nitric acid absorbs NO in the top part I-1 of column I. Absorption is accompanied by the chemical reactions leading to the formation of a heterophase system of complex composition. In the main part of column I-2, this system is composed of seven main substances: HNO_3, H_2O, NO, N_2O_3, NO_2, N_2O_4, and HNO_2. The chemical interactions in the system under consideration

MARCEL DEKKER, INC.
270 Madison Avenue, New York, New York 10016

can be described by the following four independent reactions:

$$NO + NO_2 = N_2O_3 \quad (3)$$

$$2NO_2 = N_2O_4 \quad (4)$$

$$N_2O_3 + H_2O = HNO_2 \quad (5)$$

$$N_2O_4 + H_2O = HNO_2 + HNO_3 \quad (6)$$

Therefore, the system under study can be characterized by the formal content of only three independent components and can be represented on the Gibbs-Rosebomm triangular diagram as shown in Fig. 2. It is expedient to choose H_2O, N_2O_3, and N_2O_5 as independent components and to use the formal molar fractions $X_{H_2O}, X_{N_2O_3}, X_{N_2O_5}$ $(X_{H_2O} + X_{N_2O_3} + X_{N_2O_5} = 1)$ as the parameters to describe the liquid phase composition. Here, X_{H_2O} value refers to both free and chemically-bound water. The molar fractions of components containing N(III) and N(V) are connected with the mean valence of nitrogen atoms, n, according to the following relation:

$$n = \frac{3X_{N_2O_3} + 5X_{N_2O_5}}{X_{N_2O_3} + X_{N_2O_5}} \quad (7)$$

At low temperatures the system under consideration disintegrates into three phases. The chemical absorption of NO by nitric acid is accompanied by the formation of two different immiscible liquid phases coexisting with the gas phase in

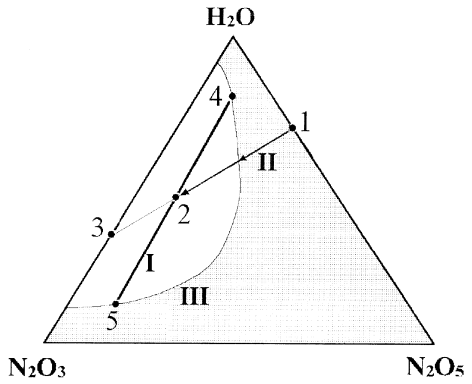

Figure 2. Triangular diagram. I, node of miscibility gap; II, trajectory of NO absorption by nitric acid process; III, boundary of miscibility gap. Shadowed area shows compositions corresponding to existence of one liquid phase; unshadowed area shows bulk compositions corresponding to co-existence of two liquid phases. Points: composition of initial nitric acid (1); bulk composition of liquids in column (2); composition of hypothetical liquid phase formed by complete reduction of nitric acid (3); compositions of light (4) and heavy (5) liquid phases.

a wide range of compositions of two liquids. Figure 2 shows schematically the transformations proceeding in the system. The region of bulk compositions where the system disintegrates into two liquid phases adjoins to the side $N_2O_3 - H_2O$ of the diagram. When NO is absorbed by nitric acid in the exchange column the composition of the liquid flow changes from point 1 corresponding to initial nitric acid to point 2 describing bulk composition of resulting flow of two liquid phases. Disintegration of the liquid flow into two liquid phases is described by the linear node of the miscibility gap. The end points 4 and 5 of the node show the compositions of the light and the heavy liquid phases. Both liquid phases are to be characterized by the analogous sets of composition parameters: X'_{H_2O}, $X'_{N_2O_3}$, $X'_{N_2O_5}$, n' for the light, and X''_{H_2O}, $X''_{N_2O_3}$, $X''_{N_2O_5}$, n'' for the heavy liquid phases, respectively (the same superscripts will be used further in the text to denote some other parameters of two liquid phases).

Due to the different densities of liquid phases the heavier liquid flows in the column a bit faster than the lighter one. It is important to distinguish two possible modes of determination of the mean concentrations of a given component in the liquid mixture flowing downwards in the column. The first mode deals with the estimation of the mean content of a component in the entire amount of the liquid mixture occurring in a thin cross-sectional layer of the column by using the following expression:

$$\overline{X} = (\rho' X' + \rho'' X'')/(\rho' + \rho'') \tag{8a}$$

where X' and X'' are the molar fractions of the same component in the lighter and in the heavier liquids, respectively; ρ' and ρ'' are the hold-up of nitrogen by corresponding liquid phases. The second mean characteristic is the mean content of the same component in the entire flow of the liquid mixture passing through a given cross-section of the column, which can be determined as:

$$\widetilde{X} = (L'X' + L''X'')/(L' + L'') \tag{8b}$$

where L' and L'' are the flow densities of the liquid phases (mg-atom of nitrogen per cm^2 of the cross-sectional area of the column per min).

Similarly, two different methods to define the mean valences $\bar{n}$ and $\tilde{n}$ of nitrogen, the mean atomic fractions $\bar{x}$ and $\tilde{x}$ of ^{15}N, the mean total concentrations $\overline{C}$ and $\widetilde{C}$ of two nitrogen isotopes ^{14}N and ^{15}N in the liquid flow, and the separation factors $\bar{\alpha} = \bar{x}/y$ and $\tilde{\alpha} = \tilde{x}/y$ can be applied. Here y is the atomic fraction of ^{15}N in the gas phase. It is convenient to introduce the individual equilibrium separation factors for the isotope exchange between lighter liquid and the gas phases

$$\alpha' = x'/y \tag{9a}$$

and between the heavy liquid and the gas phases:

$$\alpha'' = x''/y \tag{9b}$$

MARCEL DEKKER, INC.
270 Madison Avenue, New York, New York 10016

where x', x'', and y are the atomic fractions of ^{15}N in the equilibrated light liquid, heavy liquid, and the gaseous phases, respectively. Then the bulk separation factor $\tilde{\alpha}$ can be expressed by the following equation:

$$\tilde{\alpha} = \frac{a'L' + a''L''}{L' + L''} \tag{10a}$$

After rearrangement of the last equation by accounting for analogous interrelation between $\tilde{n}$, n', and n'' values one obtains

$$\tilde{\alpha} = a'\frac{\tilde{n} - n''}{n' - n''} + a''\frac{n' - \tilde{n}}{n' - n''} \tag{10b}$$

The bulk separation factor $\tilde{\alpha}$ is a more important parameter than $\bar{a}$ because it determines the steady-state mass-balance in the separation column, which is described as follows:

$$L\tilde{x} - Gy = (L - G)\, x_P \tag{11}$$

where $L = L' + L'' = L_o(1 + s)$ and G are the flow densities of the liquid and of the gas phases in the main part of the exchange column; s is the parameter of NO absorbability in HNO_3; x_p is the atomic fraction of ^{15}N in the product flow, P, where $P = L - G$. Taking into account that absorption of NO by HNO_3 flow is accompanied by decreasing of nitrogen valence from 5 to some mean value $\tilde{n}$, the absorbability parameter s can be expressed as follows:

$$s = (L - L_o)/L_o = (5 - \tilde{n})/(\tilde{n} - 2) \tag{12}$$

The most important characteristics of the separation process is the degree of ^{15}N extraction from the initial nitric acid, Γ, which is defined as follows:

$$\Gamma = Px_p/Lx_o \tag{13}$$

and the productivity, j, described by the following relationship:

$$j = Px_p = \Gamma Lx_o \tag{14}$$

(here x_o is the atomic fraction of ^{15}N in the initial nitric acid), which depend on the nitrogen oxide absorbability, s. According to Safonov and Larikov (34), in the low temperature NITROX-system with the additional absorption of gas by the liquid flow the maximum degree of ^{15}N extraction from the initial nitric acid, (Γ_{max}, and the maximum productivity, j_{max}, (in the infinitely long column) can be expressed by the following equations:

$$\Gamma_{max} = (\tilde{\alpha} - 1)(1 + s) \tag{15}$$

$$j_{max} = \Gamma_{max}L_o x_o = (\tilde{\alpha} - 1)(1 + s)L_o x_o \tag{16}$$

MARCEL DEKKER, INC.
270 Madison Avenue, New York, New York 10016

EXPERIMENTAL STUDY OF LOW-TEMPERATURE NITROX PROCESS. SET-UP AND EXPERIMENTAL TECHNIQUES

Experimental Set-Up

Schematic diagram of the apparatus used in this study is shown in Fig. 3. The main parts of the unit were manufactured with the Pyrex glass. The apparatus comprises several sections (I-1, I-2, and I-3) including the packed exchange col-

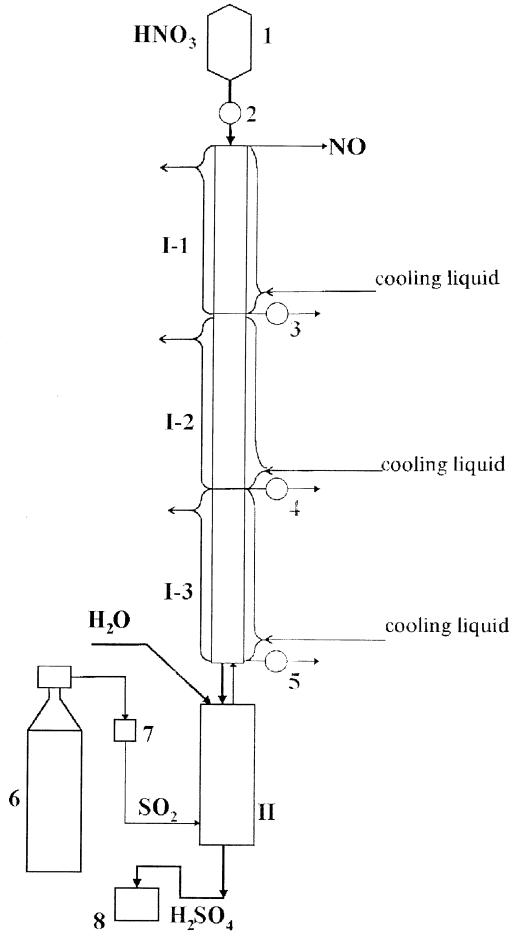

Figure 3. Schematic diagram of experimental set-up. I-1, I-2, and I-3 sections of low-temperature exchange column; II, refluxing column; 1, initial nitric acid feed-tank; 2, needle valve; 3, 4, and 5, Teflon valves; 6, SO_2 supply bottle; 7, regulating valve; 8, H_2SO_4 tank.

MARCEL DEKKER, INC.
270 Madison Avenue, New York, New York 10016

umn I and the supplementary systems II designed to reduce the liquid flow of mixture of the nitric acid and nitrogen oxides to the gaseous nitrogen oxide (II). The exchange sections (I-1, I-2, and I-3) were filled with the $0.2\times 0.2 \times 0.02$ mm stainless steel triangular helices (adjacent coils shifted by 10–20°). The helices of this type were successfully applied for decades in the former Soviet Union in industrial scale for fractionation of different isotopes (11,18). The refluxer column II was filled with the quartz helices. The exchange sections (I-1, I-2, and I-3) were supplied with two jackets. The external jacket was evacuated and the thermostating cooling liquid was circulating through the internal one. The double jacket system improved significantly the thermostating conditions of the exchange column. On the other hand, it permitted the visual following up of the process in column at low temperatures.

The liquid nitric acid was fed into the upper section I-1 from reservoir 1 through a special needle valve 2. The liquid phases along with an additional flow of demineralized water were directed from the bottom of the exchange column into the top part of the refluxer column II. The flow of gaseous SO_2 was fed through the regulating valve 7 to the bottom part of column II from SO_2 supplying tank 6. The refluxer was cooled with water flow (at 283–288 K) through the thermostating jacket. The position of the reaction zone in the refluxer was controlled visually. The gaseous mixture of nitrogen oxides (containing basically NO) was directed from the upper part of the refluxer column II to the bottom part of the exchange column counter-currently to the flow of liquid phases. The gas leaving the exchange column was not refluxed. The Teflon valves 3, 4, and 5, installed between sections I-1, I-2, and I-3 (see Fig. 3) and between exchange column I and the refluxer II, permitted collection of samples of the gas phase for the analysis of ^{15}N content.

The set-up shown in Fig. 3 was used both in experiments on isotopes separation and for investigations of the equilibrium and dynamic characteristics of the isotope exchange system. In different experiments the number of the exchange sections, their heights and diameters were varied.

Chemical Interactions of Liquid Nitric Acid with Gaseous Nitrogen Oxides at Low Temperatures

The chemical composition of the liquid and gaseous phases was determined from the results of the analysis of samples withdrawn from the middle part of the exchange column far enough from its top and bottom ends. For this purpose the middle section of exchange column (I-2 in Fig. 3) was replaced with a specially constructed liquid flow sampler III shown in Fig. 4. This made it possible to direct (by means of magnetic distributor III-1) the whole flow of the liquid phases from the upper exchange section I-1 to either the lower exchange section I-3 (during the main period of the process) or into the thermostated calibrated volume III-4 (for a short period of ~0.5–1.0 min). Then the collected liquids were separated

MARCEL DEKKER, INC.
270 Madison Avenue, New York, New York 10016

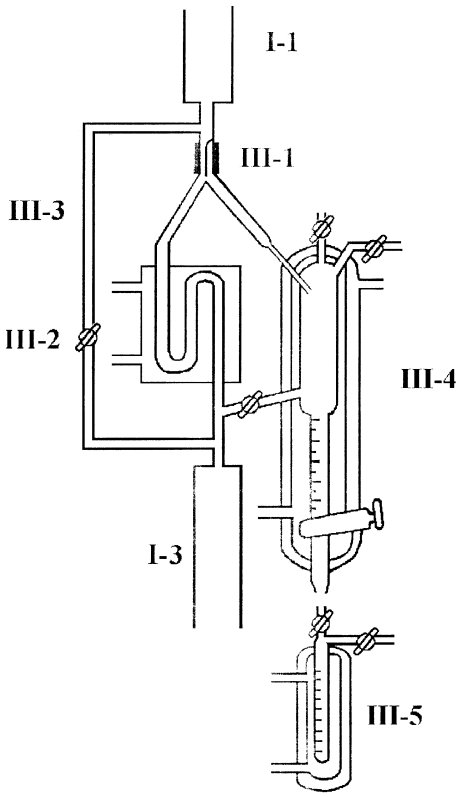

Figure 4. Schematic diagram of liquid-flow sampler. I-1 and I-3, packed exchange sections; III-1, magnetically operated distributor; III-2, gas-flow lock; III-3, the tube for the gas flow; III-4 and III-5, calibrated thermostated volumes.

to two different liquid phases of known volumes followed by the determination of their chemical compositions.

The length of the top part of exchange column where the absorption of the gaseous NO by the liquid flow of nitric acid occurred was estimated in a series of experiments with different heights of the exchange section I-1 above distributor III-1 (see Fig. 4) and with different values of the feed-flow of nitric acid. The influence of composition of the gas flow from refluxer on the equilibrium compositions of phases in the exchange column was evaluated in a series of experiments with different content of the NO_2 (N_2O_4) oxides in the gas phase. The variation of the gas phase composition was achieved by decreasing the water flow in the top part of refluxer.

Equilibrium of Nitrogen Isotopes Exchange

The determination of separation factors α' and α'' (see Eqs. 9a and 9b) at low temperature was carried out by using the same liquid flow sampler III shown in Fig. 4. The liquid flow from the exchange section I-1 was collected during a short period (~0.5–1 min) in the thermostated volume III-4 (see Fig. 4) and then without separation of individual liquid phases it was stirred for about 6 hours to achieve the isotope-exchange equilibrium. During this time the ^{15}N content in the gas phase was periodically analyzed. After equilibration both liquid phases were either analyzed as a whole or separated as above, and the ^{15}N content in both liquid and gaseous phases was measured. This series of experiments was performed by using the partial refluxing regime for the liquid flow to prevent the influence of the ^{15}N accumulation in the column on the values of equilibrium parameters. The α' and α'' values were determined in the temperature range between 254.5 and 231 K for the concentration of the initial nitric acid from 11.0 to 16.5 M.

Dynamic Characteristics of Isotope-Exchange Column

Dynamic characteristics of the low-temperature NITROX process under study were studied by using two different experimental approaches.

The first approach was based on the "pulse" method described in detail elsewhere (35–40). This approach permits the simultaneous determination of up to 3–4 parameters of the isotope-exchange column. The method is based on the mathematical treatment of the experimental concentration-time histories representing the response to a disturbance of the ^{15}N concentration obtained in a certain cross-section point of the exchange column. The apparatus used in these experiments differs from that shown in Fig. 3 only by construction of the exchange column consisting, in this case, of five sections. The apparatus operated in the incomplete-reduction-of-the-liquid-nitrogen-compounds regime in the refluxer so that the fractionation of the nitrogen isotopes did not occur and the ^{15}N concentration in the liquid flow in each cross-section of the exchange column was the same as that in the initial nitric acid. The pulse of ^{15}N concentration was introduced by injecting 0.2–0.3 ml of 8.5 M nitric acid with the ^{15}N content of 97 atom % between two upper sections of the exchange column. The distance between injection point and the bottom end of the exchange column, z_o, was constant in all cases and equaled 224.5 cm. Due to the incomplete refluxing of the liquid flow the ^{15}N concentration disturbance was gradually moving downwards.

After introduction of ^{15}N pulse the samples of gaseous nitrogen oxide were periodically collected from the Teflon valves positioned between the exchange sections at distances of 60.5, 115.5, 171.0, and 224.5 cm from the bottom end of the exchange column and analyzed by using a mass-spectrometer. The overall

MARCEL DEKKER, INC.
270 Madison Avenue, New York, New York 10016

amount of ^{15}N collected for analysis did not exceed 4–5% of ^{15}N quantity introduced into the column. Experimental elution curves were treated by using the following mathematical models of the mass-exchange process in the column:

1) the equilibrium diffusion model (ED)

$$\frac{\partial y}{\partial t} = -u\frac{\partial y}{\partial z} + \frac{E}{\rho}\cdot\frac{\partial^2 y}{\partial z^2} \tag{17a}$$

$$\tilde{x} = \tilde{\alpha}y \tag{17b}$$

2) the non-equilibrium model of plug flow (PF)

$$\chi_L\widetilde{C}_L\frac{\partial\tilde{x}}{\partial t} = L\frac{\partial\tilde{x}}{\partial z} + k_G(y - \tilde{x}/\tilde{\alpha}) \tag{18a}$$

$$\chi_G C_G\frac{\partial y}{\partial t} = -G\frac{\partial y}{\partial z} - k_G(y - \tilde{x}/\tilde{\alpha}) \tag{18b}$$

where $u \equiv (G - \tilde{\alpha}\tilde{L})/p$ is the velocity of movement of the mass-center of ^{15}N pulse, cm/min; $\rho \equiv \tilde{\alpha}\chi_L\widetilde{C}_L + \chi_G C_G$; $E \equiv \tilde{\alpha}E_L + E_G$ is the bulk coefficient of axial dispersion, mmol/cm · min; E_G and E_L are the coefficients of axial dispersion in the gas and the liquid flows, respectively, mmol/cm · min; C_G is the total concentration of ^{14}N and ^{15}N in the gas phase, mg-atom N/cm^3; $\widetilde{C}_L$ is the mean total concentration of ^{14}N and ^{15}N in the liquid flow, mg-atom N/cm^3; χ_G and χ_L are the volume fractions of the gas and the liquid in column.

The solution of the ED model describing the broadening of a δ-like ^{15}N pulse is as follows (35–37):

$$y(z,t) = y_o + \frac{Q}{2\sqrt{\pi\rho Et}}\exp\left\{-\frac{\rho[(z - z_o) - ut]^2}{4Et}\right\} \tag{19}$$

where Q is the injected quantity of ^{15}N per 1 cm^2 of the cross-sectional area of the column; y_o is the initial atomic fraction of ^{15}N in the gas phase.

The solution of Eqs. (18a)–(18b) of the PF model for a very narrow signal by assuming that $\chi_G C_G/\chi_L\widetilde{C}_L \to 0$ has the following form (40):

$$y(z,t) = y_o + \frac{Qk_G}{\alpha\chi_L\widetilde{C}_L G}\cdot\exp\left\{-\frac{z - z_o + w_L t}{G/k_G} - \frac{k_G t}{\tilde{\alpha}\chi_L\widetilde{C}_L}\right\} \times I_o\left(2\sqrt{\frac{k_G^2(z - z_o + w_L t)t}{\tilde{\alpha}\chi_L\widetilde{C}_L G}}\right) \tag{20}$$

where I_o is the zero-modified Bessel function, $w_L = L/\chi_L\widetilde{C}_L$. It has been shown by Safonov et al. (37) that the dynamic parameter of the ED model, $h_E = E/L$, is connected with the height of the transfer unit (HTU), $h_G = G/k_G$, being the parameter of the PF model as $h_E = \tilde{\alpha}h_G$. If $\tilde{\alpha} \approx 1$, both dynamic character-

MARCEL DEKKER, INC.
270 Madison Avenue, New York, New York 10016

istics are equal to each other and are also equal to the height of equivalent theoretical stage (HETS).

The model parameters were determined from the experimental response curves by using the random search method through minimization of the following function:

$$\psi = \frac{\sum_{i=1}^{Z} [(y/y_o)_{i,\text{exper.}} - (y/y_o)_{i,\text{theor.}}]^2}{[(y/y_o)_{i,\text{exper.}} \cdot (y/y_o)_{i,\text{theor.}}]} \tag{21}$$

where $(y/y_o)_{i,\text{exper.}}$ and $(y/y_o)_{i,\text{theor.}}$ are the experimental and the calculated values, respectively, standing in Eqs. (19) or (20) for i-sample of the gas phase and Z is the number of experimental points.

The second approach was based on the analysis of the steady-state concentration of ^{15}N in the refluxing flow of the separation unit. The exchange column consisted of either 4 or 5 sections and was working under complete-refluxing-of-the-liquid-flow mode of operation. The isotopic composition of the gas flow leaving the refluxer was analyzed periodically until achieving the constant value. The enriching factor q in the steady state is determined as follows:

$$q_{st} = y_{R,st}/x_o \tag{22}$$

where $y_{R,st}$ is the steady-state atomic fraction of ^{15}N in the gas flow leaving the refluxer and x_o is the atomic fraction of ^{15}N in the initial nitric acid. The HETS values were determined from the respective q_{st} values by using the following equation (41):

$$q_{st} = \exp\frac{(\bar{\alpha} - 1)H}{h} \tag{23}$$

where H is the total height of the exchange column, and h is the HETS. For comparison, the experiments were carried out both at room and low temperatures.

Enthalpy of Absorption of Nitrogen Oxide by Nitric Acid

The enthalpy of absorption of nitrogen oxide by nitric acid was estimated from experimental data obtained in the counter-current column. The construction of exchange column consisted of three thermostated sections (each 40–42 cm in height with a diameter of 1.5 cm) was nearly analogous to that shown in Fig. 3. The exit of gas flow from the column (through valve 3) was located between the upper and middle sections. The absorption of nitrogen oxide by nitric acid occurred in this case in the middle exchange section. The thermostated conditions were provided by circulation of a cooling agent (ethanol) through the thermostat-

MARCEL DEKKER, INC.
270 Madison Avenue, New York, New York 10016

ing jacket of the middle section. The temperature of the coolant was measured continuously before entering the jacket and after leaving it. The difference in these temperatures ΔT allowed for estimation of the enthalpy of absorption of nitrogen oxide by nitric acid using the following equation:

$$\Delta_{abs}H(T) = -\frac{v d_{eth} c_{p,eth}(T)}{M_{eth} \cdot 1000} \cdot \frac{\Delta T}{L_o} \tag{24}$$

where $d_{eth} = 0.821$ g/cm^3 is the density of ethanol; v is the rate of ethanol flow; $c_{p,eth} = 113$ J/mol · K is the specific heat capacity of ethanol.

RESULTS AND DISCUSSION

Chemical Equilibrium

The results of experiments carried out with different heights of the exchange section above the liquid flow sampler III (see Fig. 4) and with different values of the feed flow of nitric acid are presented in Table 1. As seen, the mean chemical composition of the samples of liquid collected is nearly constant (see last two columns). This means that the height of the top part of exchange column, where the absorption of the gaseous NO by HNO_3 solution occurs, does not exceed 40 cm.

Another series of experiments was carried out with different contents of NO_2 (N_2O_4) (from 0 to 20%) in the gas flow leaving refluxer. The constancy of composition of both the liquid and the gas phases was observed in this case in the middle part of the exchange column. This result confirms that all nitrogen oxides except NO almost completely condense in the bottom part of the low-temperature exchange column and then return back with the liquid flow in the refluxer. In the main part of the exchange column, the gas phase contains NO with the minimum

Table 1. Chemical Composition of Samples of Liquid Flow Collected from Exchange Column ($T = 234$ K; Concentration of initial $HNO_3 = 12.2$ M)

No.	H, cm	Diameter, cm	L_o, mg-atom N/cm^2 min	L, mg-atom N/cm^2 min	$\tilde{n}$	$\frac{\tilde{X}_{N_2O_3}}{\tilde{X}_{N_2O_3} + \tilde{X}_{N_2O_5}}$
1	40	2.35	3.0	4.7	3.60	0.70
2	40	2.35	5.4	10.2	3.58	0.71
3	40	1.5	9.9	20.1	3.60	0.70
4	40	1.5	15.7	23.6	3.56	0.72
5	100	1.7	9.5	18.4	3.55	0.73
6	100	1.7	9.8	19.5	3.58	0.71

Marcel Dekker, Inc.
270 Madison Avenue, New York, New York 10016

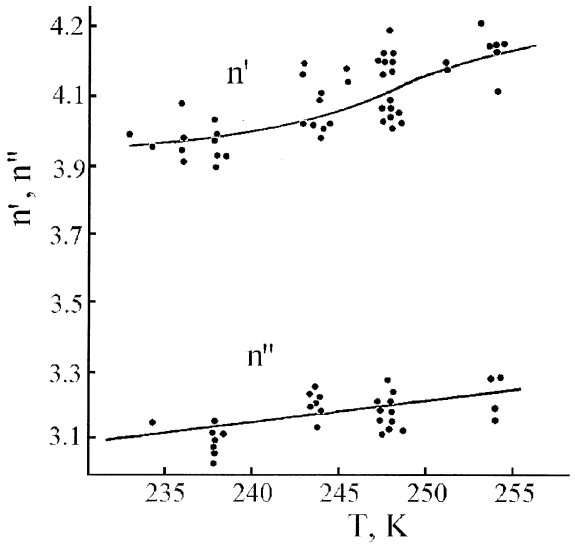

Figure 5. Dependence of mean nitrogen valences in liquid phases on temperature. n' and n'' refer to light and heavy liquids, respectively.

admixture (3–5%) of other oxides. This indicates that the chemical equilibrium in the exchange column does not depend on the conditions in the refluxer.

The experimentally determined compositions of the liquid phase samples collected from the exchange column are presented in Figs. 5 and 6 and are also partly repeated in Tables 2 and 3. These results indicate that the chemical compositions of both liquid phases do not depend on the concentration of initial nitric acid and on the flow density. Water is the main component of the light liquid phase (H_2O molar fraction = 85.2–87.6%) whereas in the heavy liquid phase, the molar fraction of water is far lower (5–6%). A decrease of temperature from 254 to 231 K leads to a slight decrease of the mean valences of nitrogen in both liquid phases. The light liquid phase can be represented as an aqueous solution of HNO_3 with some admixture of N_2O_3. The heavy liquid phase can be considered to be composed of the liquid N_2O_3 with some admixtures of HNO_3 without free water molecules. The results shown in Tables 2 and 3 indicate that the concentration of nitrogen in the heavy liquid phase (see m'' values in Table 3) is more than two times higher than that in the light liquid phase (see m' values in Table 2). The fraction of the heavy liquid phase increases with the increase of the concentration of initial nitric acid and the decrease of temperature.

The experimental results obtained by studying chemical equilibrium in the temperature range from 254.5 to 231 K have been interpolated by using the fol-

MARCEL DEKKER, INC.
270 Madison Avenue, New York, New York 10016

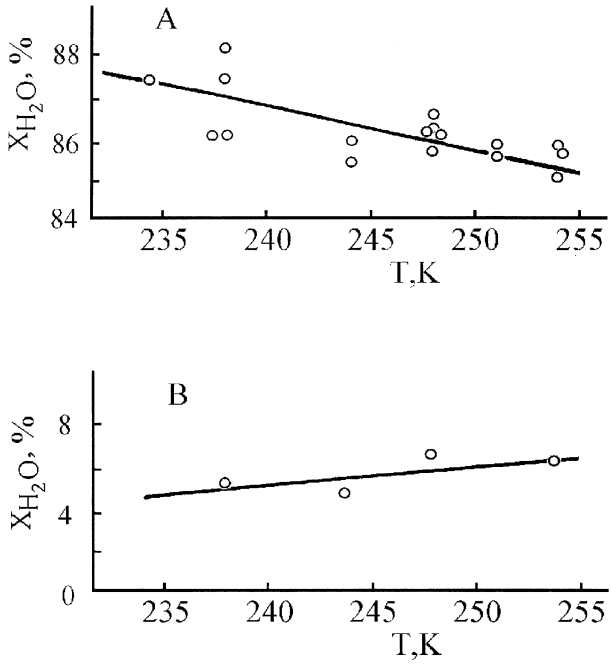

Figure 6. Molar fraction of water in light (A) and heavy (B) liquid phases at different temperatures.

Table 2. Chemical Composition of Light Liquid Phase

No.	T, K	C_{O,HNO_3}, M	L_o, mg-atom N/min · cm^2	n'	m' mg-atom N/cm^3
1	254	11.7	17.5	4.24	14.0
2	253	16.3	18.5	4.30	12.5
3	247.5	11.7	17.0	4.03	—
4	247.5	12.3	18.5	4.04	14.0
5	247.5	14.3	22.5	4.21	14.0
6	247.5	15.8	20.5	3.93	14.0
7	247.5	16.3	14.0	4.22	—
8	247.5	16.3	21.0	4.02	12.0
9	243	14.3	18.5	4.16	13.0
10	243	16.3	16.0	4.02	13.0
11	238	11.7	17.5	3.98	—
12	238	11.7	17.5	3.90	13.1
13	238	11.7	17.5	3.93	12.8
14	234.5	11.7	17.0	3.96	11.9
15	231	12.3	17.4	3.96	—

Table 3. Chemical Composition of Heavy Liquid Phase

No.	T, K	C_{OHNO_3}, M	L_o, mg-atom N/min · cm^2	n''	m'' mg-atom N/ml
1	254	16.3	—	3.19	27
2	247.5	15.8	31.6	3.18	33
3	247.5	16.0	24.0	3.17	33
4	247.5	14.0	21.0	3.29	33
5	244	16.0	24.0	3.19	33
6	238	14.0	18.2	3.09	31
7	238	14.0	21.0	3.08	—
8	234.5	14.0	—	3.22	30

lowing equations:

$$n' = 4.51 - 0.22\frac{T-273}{247.5} - 0.374\left(\frac{T-273}{247.5}\right)^2 + 0.186\left(\frac{T-273}{247.5}\right)^3 \quad (25)$$

$$X'_{H_2O} = 83.0 + 2.8\left(\frac{T-273}{247.5}\right) \quad (26)$$

$$n'' = 3.33 - 0.132\left(\frac{T-273}{247.5}\right) \quad (27)$$

$$X''_{H_2O} = 7.5 - 1.9\left(\frac{T-273}{247.5}\right) \quad (28)$$

The curves in Figs. 5 and 6 were calculated through the use of Eqs. (25)–(28).

By using Eqs. (25)–(28) for the temperature range from 254.5 to 231 K at a pressure of 1 atm, one can draw the nodes of miscibility gap in the Gibbs-Rosebomm triangular diagram shown in Fig. 7 for 253, 247.5, 243, and 234 K.

The relative quantities of two liquid phases and the bulk valence of nitrogen $\tilde{n}$ in the liquid flow in column depend on the initial nitric acid concentration and on the temperature. The value of $\tilde{n}$ can be determined from the composition ($\tilde{X}_{H_2O}$, $\tilde{X}_{N_2O_5}$) corresponding to the intersection point of the node with the trajectory of the process of absorption of nitrogen oxide (II) by initial nitric acid (see Fig. 2). This trajectory is the line connecting the respective point on the H_2O-N_2O_5 side of the triangular diagram (which represents the composition of the initial nitric acid) with the analogous point on the diagram side corresponding to the

complete reduction of N_2O_5 (or HNO_3) to N_2O_3, which occurs by the following reaction:

$$N_2O_5 + 4\,NO = 3\,N_2O_3 \tag{29}$$

The molar fraction of N_2O_5 in the initial nitric acid was calculated through the use of the following equation:

$$X_{N_2O_5} = \frac{C_o/2}{C_o/2 + (1000\,d_o - C_o \cdot M_{N_2O_5}/2)M_{H_2O}} \tag{30}$$

where C_o and d_o are the concentration (mol/l) and the density of the initial nitric acid solution, and M is the molecular mass of N_2O_5 and H_2O. Each point on the H_2O-N_2O_3 side of the diagram was calculated by using the following equation:

$$X_{N_2O_3} = \frac{3X_{N_2O_{5,o}}}{1 + 2X_{N_2O_{5,o}}} \tag{31}$$

where $X_{N_2O_{5,o}}$ is the molar fraction of N_2O_5 in the initial nitric acid, and $X_{N_2O_5}$ is the molar fraction of N_2O_3 in a hypothetical mixture formed by the complete reduction of N_2O_5 (or HNO_3) to N_2O_3. The variation of the liquid composition in the column due to absorption of NO corresponds to the shift of the point along the trajectory from the right to the left until it intersects the node of miscibility gap.

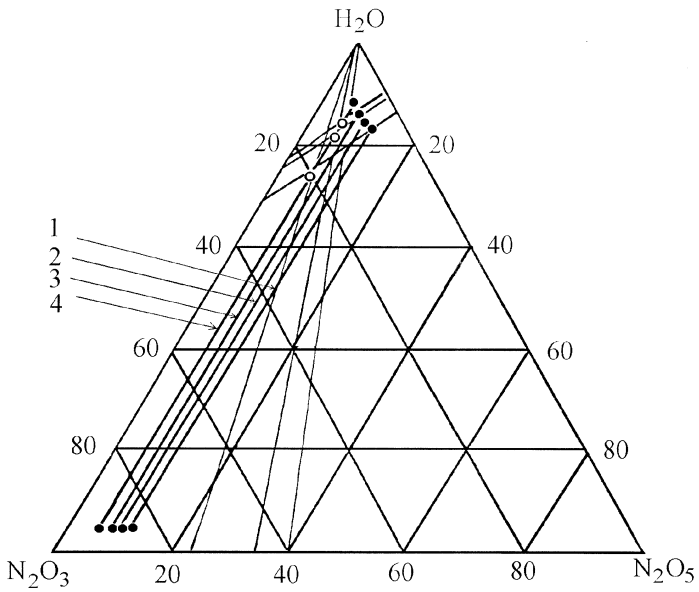

Figure 7. Experimental nodes of miscibility gap in low-temperature NITROX system at 253 K (1), 247.5 K (2), 243 K (3), and 234 K (4).

MARCEL DEKKER, INC.
270 Madison Avenue, New York, New York 10016

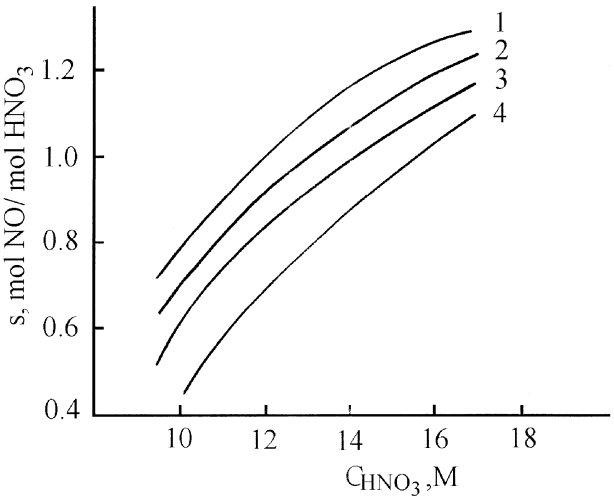

Figure 8. Absorbability of NO in nitric acid vs. HNO_3 concentration at 233 K (1), 238 K (2), 243 K (3), and 248 K (4).

The bulk compositions of the liquid flow in the column at 234 K for 9.0 M, 10.3 M, and 12.3 M initial nitric acid are shown in Fig. 7. The absorbability of nitrogen oxide, *s*, in nitric acid of different concentrations can be calculated by using the bulk valence of nitrogen estimated by Eq. (12). The results of these calculations are presented in Fig. 8.

Equilibrium of Nitrogen Isotopes Exchange

The time required to achieve the isotope exchange equilibrium in the system under study was found to be less than 1 h. The experimentally determined equilibrium separation factors for two liquid phases are shown in Fig.9. The values of α' and α'' do not depend on concentration of the initial nitric acid. Both α' and α'' slightly increase when the temperature decreases. Thus, α' and α'' values change from 1.066 to 1.071 and from 1.041 to 1.052, respectively, due to the changes in chemical composition of the liquid phases.

The temperature dependence of individual equilibrium separation factors (α' and α'') is complicated due to superposition of their self-dependence on temperature and temperature dependence of the mean valence of nitrogen acting in the opposite directions. Indeed, a decrease of temperature leads to an increase of separation factors whereas a simultaneous decrease of the mean valances of nitrogen

in the liquid phases results in a decrease of both α' and α'' values. The experimental results shown in Fig. 9 indicate the predominance of the first factor.

The experimental results on the determination of α' and α'' values were interpolated statistically by using the following equations:

$$\alpha' = 1.037 + 0.052\left(\frac{T - 273}{247.5}\right) - 0.020\left(\frac{T - 273}{247.5}\right)^2 \tag{32}$$

$$\alpha'' = 1.031 + 0.014\left(\frac{T - 273}{247.5}\right) \tag{33}$$

The curves in Fig. 9 were calculated by using Eqs. (32) and (33).

The dependencies of bulk separation factor $\tilde{\alpha}$ (average for the liquid flow in the column) on temperature and on concentration of initial nitric acid (see Fig. 10) were estimated by using Eqs. (10b), (25), (27), (32), and (33). The required $\tilde{n}$ values were determined from the composition (X_{H_2O}, $X_{N_2O_5}$) corresponding to the intersection point of the node of miscibility gap with the trajectory of NO absorption by the initial nitric acid (see Fig. 7), i.e.,

$$\tilde{n} = \frac{5\tilde{X}_{N_2O_5} + 3(1 - \tilde{X}_{N_2O_5} - \tilde{X}_{H_2O})}{1 - \tilde{X}_{H_2O}} \tag{34}$$

Figure 10 shows the calculated dependencies of $\tilde{\varepsilon} = \tilde{\alpha} - 1$ versus concentration of the initial nitric acid for 248, 243, and 233 K. The calculated dependen-

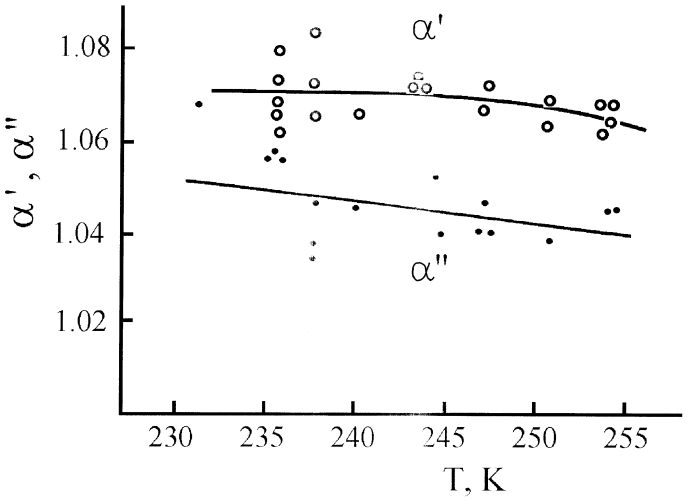

Figure 9. Temperature dependence of equilibrium separation factors for light (upper curve) and heavy (lower curve) liquid phases.

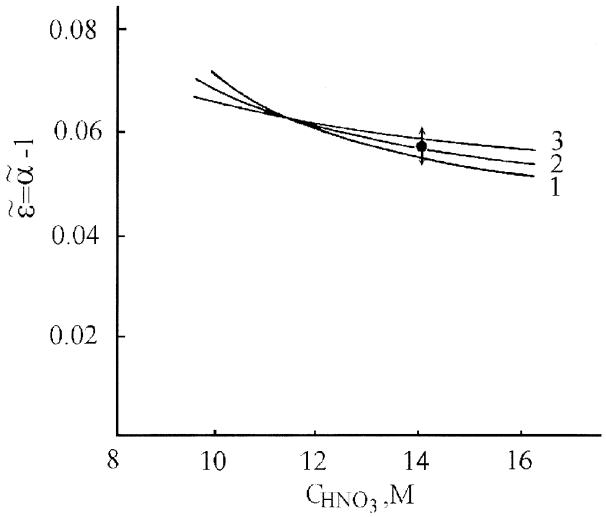

Figure 10. Dependence of bulk separation factors in column on concentration of initial nitric acid at 248 K (1), 243 K (2), and 233 K (3). Point, experimentally measured value for 14 M nitric acid at 243 K.

cies were confirmed by the direct measurement of the mean separation factor in the column at 248 K for 14 M initial nitric acid. The experimentally determined value of $\tilde{\alpha} = 1.057 \pm 0.003$ practically coincided with the calculated value $\tilde{\alpha} = 1.056 \pm 0.003$ for the same experimental conditions.

Dynamic Characteristics

Some of the experimentally obtained concentration-time histories reflecting the response to the disturbance of ^{15}N concentration in different cross-sections of the column (response-curves) are shown in Fig. 11. This series of experiments consisted of three parts: the first and the second were dedicated to determination of the dependencies of HETS values on the flow of initial nitric acid at 243 K for 11.2 M HNO_3 and at 233 K for 14.2 M HNO_3. In the third one, the dependence of HETS on concentration of the initial nitric acid at 248 K was determined.

Experimental conditions and the calculated parameters of the exchange column for one of three experimental series carried out are collected in Table 4. The dynamic characteristics of the exchange column are shown more in detail in Figs. 12 and 13. As seen in Fig. 11, the experimentally obtained response curves demonstrate a good fit with the curves calculated by both ED and PF models with

MARCEL DEKKER, INC.
270 Madison Avenue, New York, New York 10016

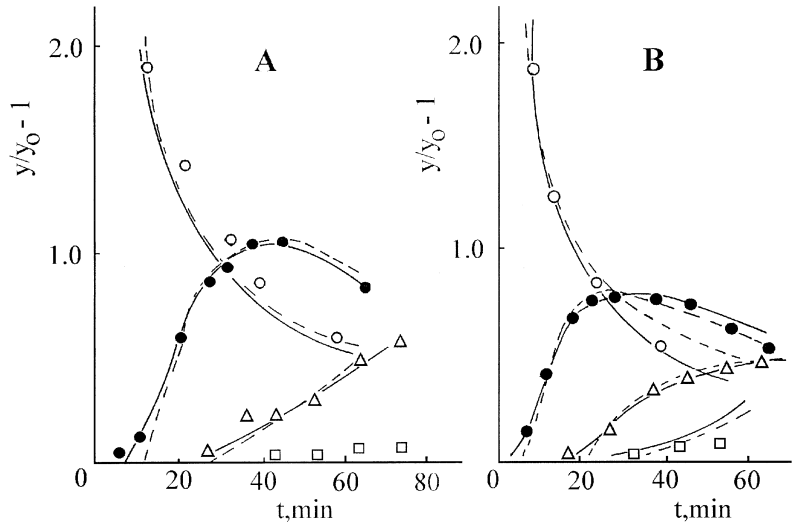

Figure 11. Curves of response to ^{15}N concentration disturbance in different cross-sections of column. Points, experiment; curves, calculated by using PF (dotted lines) and ED (solid lines) models. Conditions: (A), L_o = 12.1 mg-atom N/cm^2 · min, T = 243 K; (B), L_o = 17.8 mg-atom N/cm^2 · min, T = 243 K.

Table 4. Results of Determination of HETS by "Pulse Method" in Experiments with 11.2 M HNO_3 at 243 K

Experiment No.	1	2	3	4	5
			Experimental Parameters		
L_o	5.7	7.8	12.1	17.8	22.6
L	11.4	15.6	24.2	35.6	45.2
G	9.6	14.2	21.1	30.8	43.6
$\chi_L C_L$	3.4	4.0	4.4	5.1	5.6
			Calculation by ED Model		
h_E	2.4 ± 0.7	2.6 ± 0.6	4.2 ± 0.6	5.5 ± 0.2	6.8 ± 1.4
$\rho \cong \chi_L C_L$	4.6 ± 0.4	4.8 ± 0.2	5.5 ± 0.5	6.1 ± 0.3	6.8 ± 0.4
$-u$	1.0 ± 0.1	0.7 ± 0.1	0.8 ± 0.1	1.1 ± 0.1	0.8 ± 0.1
			Calculation by PF Model		
h_G	3.6 ± 1.1	3.6 ± 0.5	5.0 ± 0.8	7.2 ± 0.8	8.1 ± 0.6
$\chi_L C_L$	4.1 ± 0.5	4.2 ± 0.2	4.8 ± 0.4	5.0 ± 0.4	5.6 ± 0.3
G	7.6 ± 0.6	13.3 ± 0.4	21.7 ± 0.8	32.6 ± 1.2	44.1 ± 1.1

MARCEL DEKKER, INC.
270 Madison Avenue, New York, New York 10016

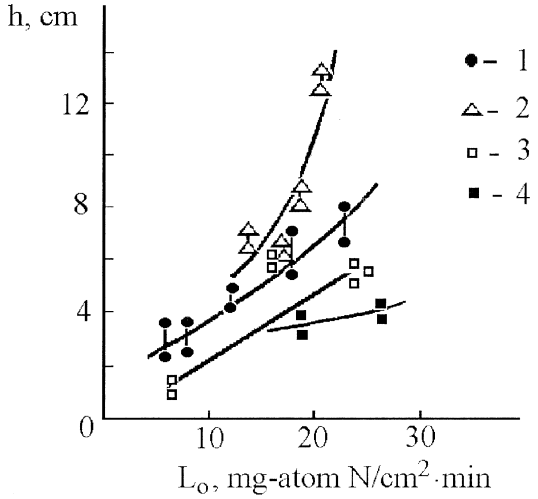

Figure 12. Dependence of HETS on initial nitric acid flow for 11.2 M HNO_3 at 243 K (1), 14.2 M HNO_3 at 233 K (2), 12.0–12.5 M HNO_3 at 248 K (3), and 14.0–14.2 M HNO_3 at 248 K (4). The upper points of each point couples was calculated by using the PF model.

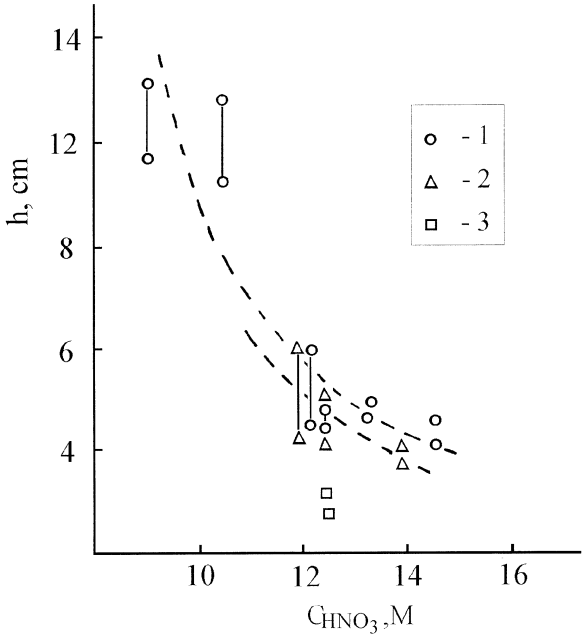

Figure 13. HETS values for 248 K plotted vs. initial nitric acid concentration at equal maximum productivity of separation column, j_{max}: $9.4 \cdot 10^{-3}$ (1), $6.9 \cdot 10^{-3}$ (2), and $2.3 \cdot 10^{-3}$ (3) mg-atom $^{15}N/cm^2 \cdot min$.

MARCEL DEKKER, INC.
270 Madison Avenue, New York, New York 10016

the use of the found meanings of system parameters. This confirms the validity of both models for description of the operation of exchange column. The calculated values of some parameters, such as G and $\rho \cong \chi_L C_L$, correlate with the experimentally determined ones (see Table 4). This coincidence demonstrates once again the reliability of the "pulse" method for determination of the dynamic characteristics of exchange column.

The differences between the calculated h_E and h_G values in all cases was within the interval of uncertainty of their determination. This correlates well with the theoretical conclusion given by Safonov et al. (37) about very small differences between h_E, h_G, and HETS values in the case of nitrogen isotope exchange.

As follows from Fig. 12, the HETS values increase from 1.5–4 cm up to 8–13 cm when the temperature decreases from 248 to 233 K. Note that the maximum HETS values of 12.8–13.2 cm were obtained near the flows range corresponding to column flooding.

To obtain the comparable HETS values in experiments with different concentrations of the initial nitric acid, its flow in each case corresponded to the maximum productivity of the separation column, which was estimated by using Eq. (16). Figure 13 shows the results of this series of experiments. As seen, the HETS values decrease dramatically with the increase of the initial nitric acid concentration.

Some of the dynamic characteristics of the low-temperature exchange column have been repeatedly determined in experiments on ^{15}N fractionation at the steady-state concentrations of ^{15}N in the gas flow leaving the refluxer of the separation unit operating under complete refluxing of the liquid flow. The experimental conditions and the steady-state separation factors determined in these experiments are presented in Table 5.

Table 5. Results of ^{15}N Fractionation in Counter-Current Column at Steady State

No.	T, K	C_{O,HNO_3}, M	H, cm	L_o^*	L^*	α	q	$(\alpha - 1)/h$	h, cm
1	293	10.2	169	11.4	11.4	1.050	19.4	0.0175	2.9
2	293	10.2	169	17.9	17.9	1.050	9.7	0.0134	3.7
3	293	10.2	169	21.1	21.1	1.050	6.99	0.0115	4.3
4	263	12.3	162	11.1	15.5	1.055	22	0.0191	2.9
5	253	10.5	190.5	13.7	21.3	1.068	10.5	0.0123	5.5
6	253	12.3	162	11.1	18.6	1.060	14.2	0.0164	3.65
7	233	12.6	162	15.2	37.3	1.062	3.2	0.00718	8.6
8	233	12.2	190.5	13.9	33.3	1.062	12.0	0.0130	4.8

* mg-at N/cm^2 min.

Marcel Dekker, Inc.
270 Madison Avenue, New York, New York 10016

The experiments carried out have shown that the low-temperature NITROX system formed by 12–14.5 M nitric acid is characterized by relatively small HETS values of 3–6 cm (at the initial nitric acid flow rate of 18–27 mg-at N/cm^2 · min). Similar HETS values are obtained as a rule by using a conventional room temperature version of NITROX method. So small HETS values observed at low temperatures are explained by fast isotope exchange between gaseous NO and liquid N_2O_3 as it has been reported earlier (42,43).

Thermochemical Characteristics of Low Temperature NITROX System

The maintenance of the low-temperature regime in the exchange column needs to provide the following conditions:

1. the preliminary cooling of the initial nitric acid flow;
2. the cooling of section I-1 of the exchange column (see Fig. 1) where the absorption of NO by nitric acid flow at low temperatures occurs;
3. the cooling of section I-3 of the exchange column (see Fig. 1) where all nitrogen oxides except NO condense from the gas flow leaving the refluxer;
4. to provide an adiabatic regime of the main part I-2 of the exchange column.

The thermochemical data for the majority of individual nitrogen compounds can be found in the literature for a wide temperature range (44–53). Although these data refer mainly to the temperatures above 273 K, they can be used to estimate the thermochemical characteristics of the low temperature NITROX system. For example, the specific heat capacity c_p (per 1 gram of solution) of aqueous nitric acid solutions of different concentrations (49) slightly decrease (within less than 1.5%) when the temperature decreases from 294 to 275 K. Although analogous data for the lower temperatures are not available in the literature, it seems reasonable to suppose that the variation of c_p at lower temperatures is also small. Hence, to estimate the enthalpy of cooling of the initial nitric acid, ΔH_{cool}, from 298 to 248 K, one can neglect these variations of c_p and use a constant value corresponding to specific heat capacity of nitric acid of a definite concentration at 275 K. The estimated values of ΔH_{cool} for the 12 M, 14 M, and 16 M HNO_3 solutions are presented in Table 7.

The enthalpy of absorption of NO by nitric acid at low temperatures was not previously determined. This quantity can be estimated through the use of molecular compositions of both liquid phases (light and heavy, see above) and the thermochemical data for the individual nitrogen compounds. The formation of both

MARCEL DEKKER, INC.
270 Madison Avenue, New York, New York 10016

phases can be described by the following reactions:

$$HNO_3 + 0.4NO = 0.8\ HNO_3 + 0.3\ N_2O_3 + 0.1\ H_2O \quad (35)$$

$$HNO_3 + 1.5NO = 0.25\ HNO_3 + 1.125\ N_2O_3 + 0.375\ H_2O \quad (36)$$

The ratios of nitrogen compounds in the right hand part of these reactions and coefficients were chosen to correspond to experimentally determined mean valences of nitrogen, which are equal to 4.14 and 3.2 for the light and the heavy liquid phases, respectively. By using simultaneously occurring reactions (35) and (36) one can describe the dependence of absorbability, s, of NO on concentration of nitric acid as it is shown in Fig. 8. Such a description suggests that water releasing in reaction (36) is dissolved in the light liquid phase. The overall reaction describing absorption of s moles NO in 1 M aqueous HNO_3 solution at low temperature can be written as follows:

$$HNO_3 + s\ NO = \left[\frac{1.5 - s}{1.1}\cdot(0.8\ HNO_3 + 0.3\ N_2O_3 + 0.1\ H_2O) + \frac{s - 0.4}{1.1}\cdot 0.375\ H_2O\right]_{light} + \left[\frac{s - 0.4}{1.1}\cdot(0.25\ HNO_3 + 1.125\ N_2O_3)\right]_{heavy} \quad (37)$$

Expressions in the square brackets correspond to the light and heavy liquid phases.

Estimation of the enthalpy of reaction (37) is based on the standard enthalpies of formation of individual chemical compounds, $\Delta_f H^o_{298}$, and their standard specific heat capacities, $c^o_{p,298}$. Some of these quantities taken from the references (44–53) are collected in Table 6.

To calculate the enthalpies of compound formation at a low temperature of 248 K, it is necessary to know the dependencies of specific heat capacities on temperature in the interval between 248 and 298 K. Because such data for the most liquid nitrogen compounds are not available in the literature, these dependencies have been disregarded through the use of the standard $c^o_{p,298}$ values:

$$\Delta_f H_{248} \approx \Delta_f H^o_{298} - c^o_{p,298} \cdot 50/1000 \quad (38)$$

This approximation is usually acceptable for the liquid compounds in a comparatively narrow temperature interval (47). The constancy of specific heat capacity of liquid water below its freezing-point is confirmed by the data obtained for supercooled water in the temperature interval 273–266 K and by those obtained for the water emulsion at lower temperatures up to 235 K (54). The temperature dependence of the specific heat capacity reported for the gaseous NO by Mischenko and Ravdel (50) also shows nonsignificant changes (about 1.7%) in the temperature interval from 298 to 248 K.

The standard specific heat capacity of liquid N_2O_3 also cannot be found in the literature. This quantity was calculated by using an empirical approach of ad-

MARCEL DEKKER, INC.
270 Madison Avenue, New York, New York 10016

Table 6. $\Delta_f H^o$ and $c^o_{p,298}$ Values for Nitrogen Oxides and Nitric Acid-Water Systems

Compound	$\Delta_f H^o_{298}$ kJ/mol	$c^o_{p,298}$ J/mol · K	$\Delta_f H_{248}$ kJ/mol
$NO_{(gas)}$	90.25	29.9	88.77
$NO_{2(gas)}$	33.5	37.5	—
$N_2O_{3(gas)}$	83.3	65.3	—
$N_2O_{4(gas)}$	9.6	78.7	
$N_2O_{3(liquid)}$	49.4	118*	43.5
$N_2O_{4(liquid)}$	−19.04	142.7	−
$H_2O_{(liquid)}$	−285.83	75.31	−289.60
$HNO_{3(liquid)}$	−174.1	109.9	−179.60
$HNO_3 \cdot 1\ H_2O$	−187.7	—	−193.2
$HNO_3 \cdot 2H_2O$	−194.6	—	−199.7
$HNO_3 \cdot 3H_2O$	−198.6	—	−203.2
$HNO_3 \cdot 4H_2O$	−201.1	—	−205.1
$HNO_3 \cdot 5H_2O$	−202.8	—	−206.3
$HNO_3 \cdot 7H_2O$	−204.6	—	−206.9
$HNO_3 \cdot 10H_2O$	−205.9	—	−207.0
$HNO_3 \cdot 15H_2O$	−206.6	—	
$HNO_3 \cdot 25H_2O$	−206.9	—	

* Specific heat capacity estimated in this work.

ditivity of the atomic specific heat capacities (50). The specific heat capacity of the liquid N_2O_3 was estimated from the corresponding standard value for the liquid N_2O_4 as follows:

$$c^o_{p,298}(N_2O_3) \approx c^o_{p,298}\ (N_2O_4) - c_p(O) \tag{39}$$

where the atomic specific heat capacity of oxygen $c_P(O) = 25.10$ J/g-atom.

The enthalpy of formation of nitric acid in the aqueous solution of light liquid phase (in which the composition corresponds to $HNO_3 \cdot xH_2O$) at 248 K was estimated as follows:

$$\Delta_f H_{248}(HNO_3 \cdot xH_2O) \approx \Delta_f H^o_{298}(HNO_3 \cdot xH_2O) - c_p,\ (HNO_3 \cdot xH_2O) \cdot -x\ c^o_p,\ (H_2O)] \cdot 50/1000 \tag{40}$$

where $c_p(HNO_3 \cdot xH_2O) \cdot$ is the specific heat capacity of the aqueous solution of nitric acid taken from Nikolsky (49). For the experimentally determined x value ($x = 4.89$) in the light phase, it was found that $\Delta_f H_{248}$ ($HNO_3 \cdot 4.89\ H_2O$) $= -206.3$ kJ/mol. The enthalpy of dissolution of liquid N_2O_3 in nitric acid of the light liquid phase and the enthalpy of dissolution of HNO_3 in the liquid N_2O_3 of

Table 7. Calculated Enthalpy Values

Concentration of Initial Nitric Acid, M	s	$\Delta_{cool}H_{298K\text{-}248K}$, kJ/mol	$\Delta_{abs.}H_{248}$, kJ/mol
12	0.70	−15.0	−20
14	0.88	−12.6	−26
16	1.04	−10.7	−32

the heavy liquid phase were neglected. Table 7 summarizes the calculated values of enthalpy of absorption of NO in nitric acid at 248 K.

Experimental results obtained by determination of the enthalpy of absorption of NO in 12.6 M nitric acid at 254 K are presented in Table 8. The experimentally found value $\Delta_{abs}H_{254} = -20 \pm 5$ kJ/mol was close to the calculated one of −17 kJ/mol for the same conditions. This coincidence confirms the validity of the calculation approach used and correctness of the experimental results obtained.

Optimal Conditions

Figure 14 shows the dependencies of Γ_{max} on the initial concentration of HNO_3 for different temperatures calculated by using experimental values of s and α. The maximum value of $\Gamma_{max} = 0.126$ corresponds to the maximal accessible concentration of nitric acid (16 M) and to the minimal achievable temperature above the freezing point of initial nitric acid (233 K). At the same time, the deviation of extraction degree from the maximal value for more dilute acid and for higher temperatures does not exceed 10–20%. For the low-temperature NITROX method, Γ_{max} values appear to be twice as large as the analogous ones determined

Table 8. Experimental Results on Determination of Enthalpy of Absorption of NO by HNO_3

No.	Concentration of Initial HNO_3, M	Coolant Temperature, K			Flow of Initial HNO_3, mol/min	Coolant flow rate, ml/min	$\Delta_{abs.}H_{254}$, kJ/mol
		$T_{initial}$	$T_{withdrawal}$	ΔT			
1	12.6	254.5	255.25	0.75	0.0161	170	−15.9
2	12.6	254.0	255.5	1.5	0.0139	110	−23.6

MARCEL DEKKER, INC.
270 Madison Avenue, New York, New York 10016

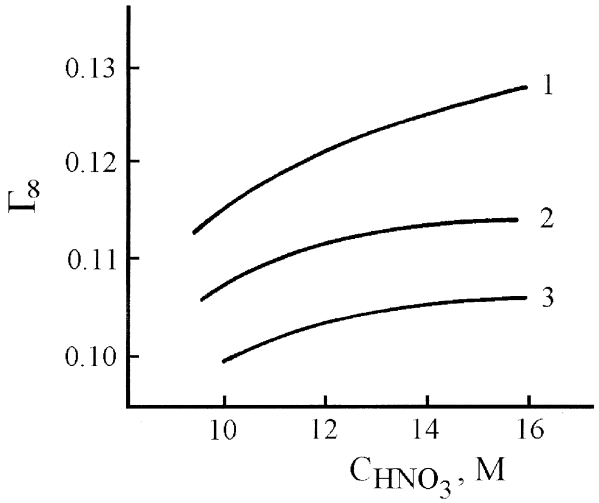

Figure 14. Calculated dependencies of ^{15}N extraction degree Γ_{max} on initial nitric acid concentration at 233 K (1), 243 K (2), and 248 K (3).

in the conventional NITROX method ($\Gamma_{max} = 0.05$). Therefore, the consumption of SO_2 per 1 unit of the ^{15}N enriched product in the low-temperature NITROX method appears to be far lower.

Any separation apparatus is characterized by the separation efficiency $A = j/H$, where H is the height of the exchange column. This parameter shows the quantity of the ^{15}N enriched product per volume unit of the exchange column. Efficiency of the separation was calculated for the column enriching ^{15}N from the natural content of 0.365% up to 5%. The separation efficiency can be calculated by using Cohen's equation (41,55), which describes the enrichment, q, of the microcomponent in the steady-state column. For the low-temperature NITROX system, this equation is written as follows:

$$N = \frac{1 + P/G}{(\tilde{\alpha} - 1)/\tilde{\alpha} + P/G} \cdot \ln \frac{q}{1 - P/G \cdot \frac{\tilde{\alpha}}{\tilde{\alpha} - 1}(q - 1)} \tag{41}$$

where q is the enrichment factor, and $N = H/h$ is the number of transfer units (NTU) or the number of theoretical stages (NTS). If $q >> 1$ and $P/G << 1$, the last equation is transformed to

$$N = \frac{\tilde{\alpha}}{\tilde{\alpha} - 1} \cdot \ln \frac{q}{1 - \frac{\tilde{\alpha}}{\tilde{\alpha} - 1} \cdot \frac{P}{L} \cdot q} \tag{42}$$

MARCEL DEKKER, INC.
270 Madison Avenue, New York, New York 10016

and then as follows:

$$j = P \cdot x_p = L(\tilde{\alpha} - 1)x_o\left(1 - \frac{q}{q_{P=O}}\right) = j_{max}\left(1 - \frac{q}{q_{P=O}}\right) \tag{43}$$

where the enrichment factor, q, in the non-productive mode of operation (without product withdrawal) is defined as follows:

$$q_{P=O} = \exp\left[\frac{(\tilde{\alpha} - 1)N}{\tilde{\alpha}}\right] \tag{44}$$

The efficiency, A, can be expressed through the use of Eq. (43) as follows:

$$A = j/H = j_{max}\left[1 - \frac{x_P/x_0}{\exp\dfrac{(\tilde{\alpha} - 1)H}{\tilde{\alpha}h}}\right]/H \tag{45}$$

where $j_{\max}$ is determined by Eq. (16).

Figure 15 shows the dependence of efficiency parameter A on the height of the exchange column, H, calculated from experimental h, $\tilde{\alpha}$, and s values of for 243 K and 11.2 M HNO_3. As seen, the A vs. H dependencies are characterized by maxima. The optimal value, A_{opt}, gradually increases with the flow of initial nitric acid. The maximal achievable A_{opt} value is determined by the flow corresponding

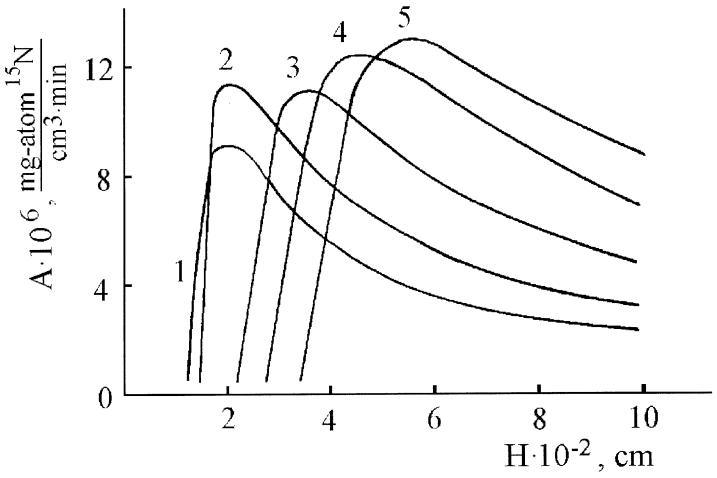

Figure 15. Dependencies of separation efficiency A on height of exchange column at 243 K for 11.2 M initial nitric acid. Initial nitric acid flow L_o (mg-atom N/cm^2 · min): 5.7 (1), 7.8 (2), 12.1 (3), 17.8 (4), 22.4 (5).

Table 9. Calculated Values of A_{opt} and H_{opt}

T, K	Concentration of Initial HNO_3, M	L_o, mg-at $N/cm^2 \cdot min$	$A_{opt} \cdot 10^6$ mg-at $^{15}N/cm^3 \cdot min$	H_{opt}, m
233	14.5	13.9	8.1–8.1	6.0
		17.4	8.3–8.3	6.3
		18.4	8.1–8.4	7.6–6.6
243	11.2	5.7	6.5–9.6	2.8–1.9
		7.8	8.9–12.3	2.8–2.2
		12.1	9.8–11.7	3.9–3.7
		17.8	10.1–13.3	5.5–4.3
		22.6	11.4–13.6	6.2–5.3
248	9.1	22.5	7.1–9.1	8.6–7.2
	10.5	24.0	6.4–9.2	8.7–7.8
	12.0	17.5	10.4–15.2	4.8–3.5
	12.2	23.8	14.9–18.5	4.9–3.9
	12.5	5.8	14.1–16.3	1.3–1.1
		17.5	13.3–15.2	4.0–3.5
		24.7	16.4–18.0	4.6–4.2
	13.4	25.0	15.5–16.3	4.9–4.5
	14.0	18.2	15.9–18.8	3.5–3.1
	14.6	26.9	19.3–22.1	4.4–3.9
298	10.2	10.0	6.1	2.3
		15.0	7.5	2.9
		20.0	8.1	3.4
		25.0	8.5	4.0

to the column flooding. This means that the comparison of apparatus efficiency for different concentrations of initial nitric acid at different temperatures must be carried out for the maximal achievable flow.

The calculated A_{opt} and H_{opt} values for different temperatures, concentrations, and flows are summarized in Table 9. The couples of A_{opt} and H_{opt} values correspond to two methods on determination of HETS based on the use of either the PF or ED dynamic model (see above). For comparison, the analogous values characterizing the conventional room-temperature NITROX method are also presented in Table 7. As seen, the maximal A_{opt} value corresponds to $T = 248$ K and 14 M HNO_3.

The comparison of the low-temperature NITROX method with its conventional version shows that for the equal flows of 25 mg-at $N/cm^2 \cdot min$ and the height of exchange columns of about 4 m, the productivity of the first method is about twice as large as that of the second one.

MARCEL DEKKER, INC.
270 Madison Avenue, New York, New York 10016

LIST OF SYMBOLS

A	parameter of separation efficiency mg-atom $^{15}N/cm^3 \cdot min$;
C	molar concentration, mol/l;
c_p	specific heat capacity, J/mol · K;
d	density of liquid, g/cm^3;
E	coefficient of axial dispersion, mmol/cm min;
G	flow density of gas phase, $mmol/cm^2 \cdot min$;
H	height of exchange column, cm;
$\Delta_{abs}H$	enthalpy of absorption of nitrogen oxide in nitric acid, kJ/mol;
$\Delta_{cool}H$	enthalpy of cooling of initial nitric acid, kJ/mol;
$\Delta_f H$	enthalpy of formation of individual chemical compound, kJ/mol;
h	height equivalent to theoretical stage (HETS), cm;
h_E	dynamic characteristics of ED model, cm;
h_G	height of transfer unit, cm;
j	productivity parameter, mg-atom $^{15}N/cm^2$ min;
k	mass-transfer coefficient in PF dynamic model, $mmol/min.cm^3$;
L	flow density of liquid phase, $mmol/cm^2 \cdot min$;
M	molecular weight;
m	concentration of nitrogen in liquid phase, mg-atom/cm3;
N	number of transfer units (NTU) or number of theoretical stages (NTS);
n	mean valence of nitrogen;
Q	quantity of ^{15}N in pulse injected in column, mg-atom $^{15}N/cm^2$ min;
q	enrichment factor;
P	density of product flow, $mmol/cm^2$ min;
s	absorbtion parameter of NO in nitric acid;
T	temperature, K;
t	time, min;
u	velocity parameter in ED model, cm/min;
v	flow rate of liquid phase, cm/min;
X	molar fraction of component;
x	atomic fraction of ^{15}N in nitrogen of liquid phase;
y	atomic fraction of ^{15}N in nitrogen of gas phase;
z	coordinate along column, cm;
α	separation factor;
Γ	degree of ^{15}N extraction from initial nitric acid;
ϵ	$\alpha - 1$;
χ	volumetric fraction of phase in column;
ρ	hold-up of nitrogen by liquid phase, mmol/ml;

Superscripts

$'$ and $''$	designate values characterizing light and heavy liquid phases, respectively;
σ	designates the standard values of the thermodynamic parameters;

MARCEL DEKKER, INC.
270 Madison Avenue, New York, New York 10016

Subscripts

eth designates values for ethanol of coolant flow;
G designates values for gas-phase flow;
L designates values for liquid-phase flow;
P designates values for product flow;
o designates flow, density, and concentration of initial nitric acid; initial atomic fraction of ^{15}N in gas phase, and column coordinate where ^{15}N concentration pulse was injected;
st designates values for steady-state mode of column operation;

Overlines

– designates mean content of component in entire amount of liquid mixture occurring in a thin cross-sectional layer of the column;
~ designates the mean content of a component in the entire flow of the liquid mixture through a given cross-section of the column.

REFERENCES

1. Benedict, M.; Pigford, T.H.; Lewi, H.W. *Nuclear Chemical Engineering,* 2nd Ed.; McGraw-Hill: New York, 1981.
2. Spindel, W.; Taylor, T.I. J. Chem. Phys. **1955**, *23*, 981.
3. Spindel, W.; Taylor, T.I. J. Chem. Phys. **1956**, *24*, 626.
4. Begun, G.M.; Drury, J.S.; Joseph, E.F. Ind. Eng. Chem. **1959**, *51*, 1035.
5. Gverdtsiteli, I.G.; Nikolaev, Yu.V.; Oziashvili, E.D. Atomn. Energ. **1961**, *10*, 487. (in Russian)
6. Axente, D.; Fodor, T. Isotopenpraxis **1969**, *5*, 267.
7. Stachewski, D. Chem. Techn. **1975**, *4*, 269.
8. Krell, E. Isotopenpraxis **1976,** *12*, 188.
9. Krell, E.; Jonas, C. In *Stable Isotopes in the Life Sciences*, Proc. of Technical Committee Meeting, Leipzig, 1977; 59.
10. Abrudean, M.; Axente, D.; Baldea, S. Isotopenpraxis, **1981**, *17*, 374.
11. Andreev, B.M.; Zelvenski, Ja.D.; Katalnikov, S.G. *Separation of Stable Isotopes by Physical-chemical Methods*; Energoatomizdat: Moscow, 1982. (in Russian)
12. Khoroshilov, A.V.; Katalnikov, S.G. Trudi Mosk. Khim. Tekhn. Inst. (Proceedings of Moscow Institute of Chemical Technology), **1984**, *130*, 18. (in Russian)
13. Foerstel, H. Isot. Environ. Health Stud. **1996**, *32*, 1.
14. Kauder, L.N.; Taylor, T.I.; Spindel, W. J. Chem. Phys. **1959**, *31*, 232.

MARCEL DEKKER, INC.
270 Madison Avenue, New York, New York 10016

15. Brown, L.L.; Begun, G.M. J. Chem. Phys. **1959**, *30*, 1206.
16. Taylor, T.; Spindel, W. In Proc. Symp. Isot. Sep., Amsterdam, 1957; North-Holland Publishing Comp: Amsterdam, 1958, 158.
17. Krell, E.; Schmidt, H.; Thiel, S. Kernenergie **1962**, *5*, 269.
18. Akopov, Yu.R.; Gverdtsiteli, I.G.; Kaminski, V.A. Partsakhashvili, G.L. Atomn. Energ. **1964**, *17*, 384. (in Russian)
19. Jonas, Ch. Isotopenpraxis **1974**, *10*, 190.
20. Khoroshilov, A.V.; Cheljak, M.M.; Katalnikov, S.G. Zh. Prikl. Khim. **1988**, *61*, 2238. (in Russian)
21. Mahenc, J. J. Chim. Phys. **1965**, *62*, 1399.
22. Mahenc, J.; Pompidor, G. Chim. Ind.-Genie Chimique **1968**, *99*, 1137.
23. Katalnikov, S.G.; Khoroshilov, A.V.; Cheljak, M.M. Atomn. Energ. **1986**, *60*, 109. (in Russian)
24. Koehret, B.; Guernier, G.; Enjalbert, M. Chem. Eng. Sci. **1973**, *28*, 735.
25. Khoroshilov, A.V. Trudi Mos. Khim. Tekhn. Inst. (Proceedings of Moscow Institute of Chemical Technology), **1981**, *119*, 138. (in Russian)
26. Khoroshilov, A.V.; Katalnikov, S.G. Isotopenpraxis **1989**, *5*, 546.
27. Katalnikov, S.G.; Sobolev, A.S.; Khachishvili, G.V.; Khoroshilov, A.V. Dokl. AN SSSR **1980**, *251*, 1190. (in Russian)
28. Katalnikov, S.G.; Sobolev, A.S.; Khachishvili, G.V.; Khoroshilov, A.V. Izv. Vuzov., Khim. and Khim. Tekhnol. **1982**, *25*, 773. (in Russian)
29. Katalnikov, S.G.; Sobolev, A.S.; Khoroshilov, A.V. Dokl. AN SSSR **1981**, *256*, 992. (in Russian)
30. Khoroshilov, A.V.; Andreev, B.M.; Katalnikov, S.G. In Proc. of Intern. Symp. on Isotope Separation and Chemical Exchange Uraniun Enrichment, Tokyo, Japan, 1990; RLNR, 486.
31. Khoroshilov, A.V. In 10th Symposium on Separation Science and Technology for Energy Applications, Gatlinburg, Tennessee, USA, 1997; Program and Abstracts, 34.
32. Khoroshilov, A.V. Khim. Prom. **1999**, *4* (241), 37. (in Russian)
33. Safonov, M.S.; Gorshkov, V.I.; Sud'in, E.V.; Gogoleva, T.V.; Chekavtsev, A.V. USSR Patent 484716, 1974.
34. Safonov, M.S.; Larikov, A.A. Teor. Osnovy Khim. Tekhnol. **1981**, *15*, 279. (in Russian)
35. Safonov, M.S.; Poteshnov, V.A.; Sud'in, E.V.; Gorshkov, V.I. Teor. Osnovy Khim. Tekhnol. **1977**, *11*, 315. (in Russian)
36. Bel'nov, V.K.; Brey, V.V.; Voskresensky, N.M.; Safonov, M.S.; Sud'in, E.V.; Trigub, L.P. Teor. Osnovy Khim. Tekhnol. **1979**, *13*, 339. (in Russian)
37. Safonov, M.S.; Larikov, A.A.; Evdokimov, S.V.; Bel'nov, V.K.; Afonina, N.I. Teor. Osnovy Khim. Tekhnol. **1982**, *16*, 604. (in Russian)
38. Safonov, M.S.; Voskresensky, N.M.; Bel'nov, V.K. ; Afonina, N.I. Teor. Osnovy Khim. Tekhnol. **1984**, *18*, 433. (in Russian)

MARCEL DEKKER, INC.
270 Madison Avenue, New York, New York 10016

39. Safonov, M.S.; Malikh, Ya.N.; Ivanov, V.A.; Gorshkov, V.I.; Bel'nov, V.K.; Voskresensky, N.M. J. Chromat. **1986**, *364*, 143.
40. Bel'nov, V.K.; Borisov, S.A.; Voskresensky, N.M.; Krjuchkova, O.L.; Modenova, V.V.; Paskonov, V.M.; Petrova, L.I.; Safonov, M.S. Teor. Osnovy Khim. Tekhnol. **1982**, *16*, 211. (in Russian)
41. Cohen, K. J. Chem. Phys. **1940**, *8*, 588.
42. Monse, E.U.; Spindel, W.; Kauder, L.N.; Taylor, T.I. J. Chem. Phys. **1960**, *32*, 1557.
43. Prencipe, M.; Spindel, W.; Ishida, T. Sep. Sci. Technol. **1985**, *20*, 489.
44. Atroschenko, V.I.; Kargin, S.I. *Technology of Nitric Acid*; Khimija: Moscow, 1970. (in Russian)
45. Atroschenko, V.I.; Perlov, E.I. *Nomogrammes in Technology of Nitric Acid*; Khimija: Leningrad, 1972. (in Russian)
46. Rossini, F.D.; Wagman, D.D.; Evans, W.H.; Levine, S.; Jaffe, I. *Selected Values of Chemical Thermodynamic Properties*, Circ. Nat. Bur. Stand., 500, Washington, 1952.
47. Karapetiants, M.Kh. *Chemical Thermodynamic*; Goskhimizdat: Moscow, Leningrad, 1975. (in Russian)
48. Glushko, V.P. *Thermal Constants of Substances*; Izd. AN USSR: Moscow, 1965, Vol. 1. (in Russian)
49. Nikolsky, B.P. *Chemist Handbook*; Khimija: Moscow, Leningrad, 1965, Vol. 3. (in Russian)
50. Mischenko, K.P.; Ravdel, A.A. *Concise Handbook of Physical-chemical Quantities*; Khimija: Leningrad, 1974. (in Russian)
51. Karapetiants, M.Kh.; Karapetiants, M.L. *Basic Thermodynamic Constants of Inorganic and Organic Substances*; Khimija: Moscow, 1968. (in Russian)
52. Glushko, V.P. *Thermal Constants of Substances*; Izd. AN USSR: Moscow, 1968, Vol. 3. (in Russian)
53. Rabinovich, V.A. *Properties of Inorganic Substances Handbook*; Khimija: Leningrad, 1983. (in Russian)
54. Franks, F. *Water and Aqueous Solutions at Temperatures below 0°C*; Naukova Dumka: Kiev, 1985. (in Russian)
55. Cohen, K. *Theory of Isotopes Separation as Applied to the Large Scale Production of U-235*; McGraw-Hill: New York, 1951.

MARCEL DEKKER, INC.
270 Madison Avenue, New York, New York 10016

Request Permission or Order Reprints Instantly!